



HAL
open science

Thermal spray alumina coatings: benefits of segmented torches for the future of plasma spraying industry?

Sleiman Myriam, Darut Geoffrey, Marie-Pierre Planche, Ralph Seulin, Gonzalez Jean-Jacques, Freton Pierre, Sambou Francis, Salito Armando, Rösli Manfred

► To cite this version:

Sleiman Myriam, Darut Geoffrey, Marie-Pierre Planche, Ralph Seulin, Gonzalez Jean-Jacques, et al.. Thermal spray alumina coatings: benefits of segmented torches for the future of plasma spraying industry?. ECHT 2024, Jun 2024, Toulouse, France. hal-04766057

HAL Id: hal-04766057

<https://ut3-toulouseinp.hal.science/hal-04766057v1>

Submitted on 4 Nov 2024

HAL is a multi-disciplinary open access archive for the deposit and dissemination of scientific research documents, whether they are published or not. The documents may come from teaching and research institutions in France or abroad, or from public or private research centers.

L'archive ouverte pluridisciplinaire **HAL**, est destinée au dépôt et à la diffusion de documents scientifiques de niveau recherche, publiés ou non, émanant des établissements d'enseignement et de recherche français ou étrangers, des laboratoires publics ou privés.

Thermal spray alumina coatings: benefits of segmented torches for the future of plasma spraying industry?

Myriam SLEIMAN, Geoffrey DARUT, Marie Pierre PLANCHE, Ralph SEULIN

UTBM, CNRS, ICB, F-90010 Belfort cedex, France

Corresponding author: myriam.sleiman@utbm.fr

Jean-Jacques GONZALEZ, Pierre FRETON, Francis SAMBOU

LAPLACE, UMR 5213 CNRS-INP-UPS, Toulouse, France

Armando SALITO, Manfred RÖSLI

Guhlfi AG, Wohlen, Switzerland

Abstract

Industries favor plasma spraying because of its combined efficiency and flexibility. Segmented plasma torches offer distinct advantages: reduce the continuous back-and-forth movement of the arc and improve the homogeneity of powder treatment. These features make them a compelling alternative to conventional turbulent torches like the F4 and 9MB.

Motivated by this potential, this paper reports a study on the microstructure of alumina coatings deposited using a segmented plasma torch. The characterization focuses on porosity, hardness, deposition efficiency and thickness. Initial results show that the segmented torch may reduce energy consumption and gas flow rate while maintaining or even improving the microstructure compared to traditional torches.

Introduction

Among established thermal spraying methods like flame, plasma, and electric arc, plasma technology stands out as the most prevalent choice within industry [1]. This is facilitated by its expansive material compatibility, encompassing even ceramics and metals boasting high melting points. Moreover, plasma offers remarkable flexibility, seamlessly adapting to existing industrial environments. This process is capable to generate a plasma jet from some centimeters to one-meter-long depending on the environment pressure. It also permits manipulation via robotic arms and empowers treatment of even large-volume components. Notably, plasma spraying offers cost-effectiveness compared to alternative methods and adheres to environmentally friendly principles.

Within a plasma torch, plasma generation occurs within a dedicated chamber composed of a tungsten tip cathode and a concentric copper anode. These electrodes serve as the focal points of an electric arc. Cold gases like argon, hydrogen, or others (nitrogen, helium...) are injected into this chamber. The interaction between the cold gas and the intense heat of the electric arc

triggers ionization, transforming the neutral gas into a highly energetic jet, ionized state forming the plasma.

The plasma jet consists of a main arc column, attached to the end of the cathode tip which is the source of the electrons, and a connecting column which terminates at the arc root on the inner surface of the anode. This generate a plasma jet exiting the torch at temperatures exceeding 12k K and velocities reaching around 2,000 m/s [2]

For several years, the industry has predominantly used the classic two-electrode torch geometry, exemplified by the PTF4 model. However, this design suffers from inherent limitations characterized by unstable and stochastic phenomena [3] [4] consisting of an erratic behavior of the electrical arc within the nozzle [5] and a persisting back-and-forth movement across the anode surface called restrike mode.

The persistent back-and-forth movement of the arc induces a significant variation in arc length. This, in turn, leads to fluctuations in the operating voltage of the torch (arc voltage). These fluctuations directly contribute to inconsistencies in particle treatment in the jet at the exit of the torch, ultimately resulting in degraded coating quality [6]. To address the challenge of arc voltage fluctuations and optimize the plasma spraying process, segmented torches were developed [7].

This new type of torch, known as a segmented torch, features a unique anode design. The anode comprises a stack of isolated copper rings insulated from each other and is defined by a conducted final ring where the arc is fixed. This configuration delivers two key advantages: reduced arc displacement and a significantly higher arc voltage compared to conventional torches. The presence of neutrodes, strategically placed between the anode and cathode, contributes to both benefits[8]. Consequently, segmented torches enable higher power levels while maintaining a minimal arc current and using lower secondary gas flow rates [9], [10], leading therefore to a longer lifespan of the electrode and a reduction in both energy and process costs.

This study seeks to evaluate the efficiency of modular Larmor segmented torches compared to the established F4 torch. These Larmor plasma torches are manufactured and marketed by Gulhfi AG (Switzerland), a company specializing in the design and development of advanced plasma processes.

To achieve this comparative study, a multi-dimensional approach will be employed. Firstly, for the same obtained net power, the microstructural properties of the alumina deposits produced by both torch types will be characterized, focusing on porosity, hardness, deposition yield and thickness. Secondly, a detailed cost analysis of the process for manufacturing the alumina coating will be conducted, considering the specific operating parameters used. Finally, the findings from both microstructural and cost analyses will be compared.

1- Materials and Processes

a. Feedstock

The feedstock used in the investigation is a commercially available Al_2O_3 Amdry 6062 powder (Oerlikon Metco, Switzerland) with a particle size distribution ranged from 22 to 45 μm presented in Figure 1. The powder flow rate in the study is 30 g/min.

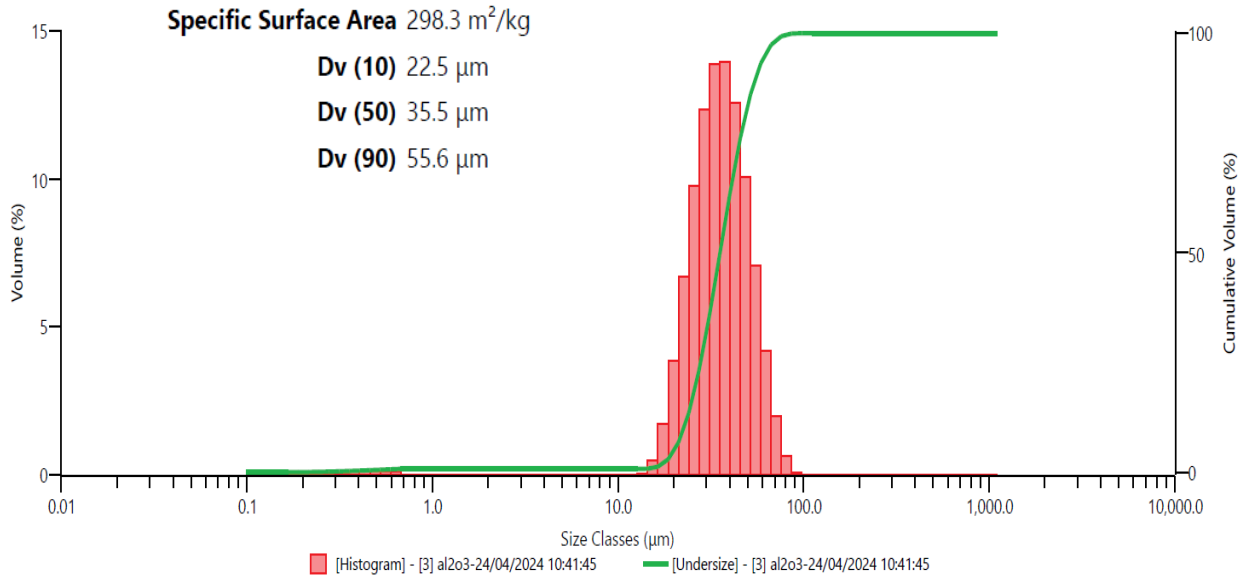


Figure 1: Distribution of alumina powder

b. Torches and Related Operating Parameters

The classical F4MB plasma torch (Oerlikon Metco Switzerland) with a 6mm diameter anode is considered as reference for comparison. Under these conditions, the mean arc voltage is 73 V, resulting in an electrical power of 47 kW, and a net power of 27 kW with a total loss of 20kW (the power loss calculation will be detailed in the next paragraph). The energy used to operate the torch is 51 kW.

For a meaningful comparison between the F4 and Larmor torches, matching the plasma energy amount is crucial. Therefore, the same net power of 27 kW is targeted across all configurations.

Using modular Larmor torch, different combinations of neutrodes and nozzle diameters are possible. Considering the objective to achieve the desired net power of 27 kW, Larmor

9 with tunnel 10 and Larmor 15 with tunnel 10 are studied as careful selection of operating parameters. The relationship between the number of neutrodes, the distance between the cathode and the anode, and the operating parameters of each torch is given in Table 1. A series of experiments were conducted to determine the operating parameters that would yield a net power equal to that obtained with the F4 torch.

Table 1: Configurations of plasma torch and operating parameters to achieve a 27 kW net power.

Torches	F4MB	Larmor 9	Larmor 15
Stacks or cathode-anode distance d (mm)	-	9 (39.1)	15 (61.8)
Anode nozzle (mm)	6	10	10
Current intensity (A)	650	450	
Ar flow rate (L/min)	40	35	
H ₂ flow rate (L/min)	12	2	
Arc voltage (V)	73	115	140
Electrical power of the torch (kW)	47	52	64
Initial electrical power (kW)	51	71	82

The coatings were sprayed on steel plates with dimensions of 40x 20 mm and 2 mm thickness. The plates were previously grit blasted with F36 corundum at a pressure of 2.5 bar to achieve a surface roughness about 3-3.5 μm . The spray distance is 110 mm from the exit of the torch to the surface of plates.

The following parameters were held constant for all deposition experiments, and are listed in Table 2:

Table 2: Constant parameters for Larmor torches

Powder mass feed rate (g/min)	30
Injector diameter (mm)	2
Substrate surface area (mm ²)	800
Carrier gas flow rate (L/min)	4
Deposition time (effective time for 14 passes)	1min 24s

c. Characterization techniques

To evaluate the energy efficiency of the Larmor torch and compare it to the F4MB torch, several characterizations are required. First, initial electrical power (the energy used to operate the torch), electrical power of the torch, net power, losses, and arc voltage will be measured to determine the operating parameters that match the F4 torch's net power, in its optimal use (in the scope of the deposition quality and efficiency) [11] as previously

mentioned. This assessment allows for evaluating the efficiency gains associated with higher voltage. Second, the microstructure of deposits obtained with these selected parameters will be examined. This analysis aims at investigating whether the Larmor torches produce coatings quality comparable or even superior to those achieved with a traditional torch.

The control panel of the system, showcased in Figure 2, displays the arc voltage, electrical power (P_e), and net power (P_n) for real-time monitoring. Net power is calculated by subtracting system losses from the total electrical power input ($P_n = P_e - \text{losses}$). These losses are determined by this formula ($\text{losses} = \dot{m} C_p (T_{\text{outlet}} - T_{\text{inlet}})$), with \dot{m} : Mass flow rate of the water (kg/s), C_p : Specified heat at constant pressure of water (J/K.kg), T_{outlet} : Temperature of the water at the outlet of the torch ($^{\circ}\text{C}$) and T_{inlet} : Temperature of the fluid at the inlet of the torch ($^{\circ}\text{C}$). T_{outlet} and T_{inlet} are also measured by the control panel. Electrical power, directly displayed on the panel, is the multiplication of voltage and current ($P_e = U.I$).

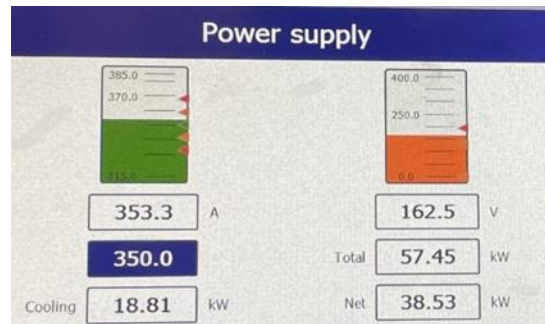


Figure 2: Control panel of the system

Detailed microstructural analysis of the as-sprayed coatings is conducted using field-emission scanning electron microscopy (FE-SEM) (JSM-7800F, JEOL, Japan) on both cross-sections and top surfaces. Cross-sectional specimens are prepared via diamond saw sectioning and resin mounting, followed by meticulous grinding with emery paper and diamond paste polishing to achieve a mirror finish. To enhance observation of the ceramic layers, all observed samples are sputter-coated with a thin layer of gold. Microhardness measurements are conducted on polished cross-sections using a Vickers indenter (Leitz, RZD-DO, Germany) with a 300 g load and 15 s holding time. Ten indentations are randomly made within different regions of each sample. ImageJ software [12] is used to calculate porosity by analyzing five randomly acquired SEM images (x200 magnification) across the entire cross-section, excluding edge regions.

The deposition efficiency was determined by calculating the ratio of the deposited mass on a cylinder (to spray all the time on a large substrate) to the mass flow rate of the powder.

The thickness of the deposited layer was initially measured using a capillary for preliminary assessment. To validate these initial measurements, an average of ten thickness measurements was obtained across the entire surface using a numerical camera (SONY) coupled to an optical microscope EPIPHOT (NIKON) with a magnification of x200.

2- Results, discussion, and comparison of coating microstructures

Coating obtained with the F4MB torch serves as the based reference for this study. As a reminder, the optimized operating parameters of the F4MB torch for depositing the alumina coating are given in Table 3. The operating parameters of segmented torches are also summarized. The comparison indicates that in both cases the voltage is higher for Larmor torches than for F4. The current intensity and secondary H₂ flow rate are reduced contributing to a longer lifespan of the electrodes. Segmented torches therefore result in reduced maintenance requirements.

Table 3: Operating parameters of the F4MB and segmented Larmor torches

Operating parameters	F4MB	Larmor 15	Larmor 9
Arc current intensity (A)	650	450	
Ar flow rate (L/min)	40	35	
H ₂ flow rate (L/min)	12	2	
Arc voltage (V)	74	115	140
Net Power (kW)	27		

Figure 3 shows the microstructure of the reference alumina deposit using F4MB. The reference alumina coating possesses a porosity of 2.8 %, a microhardness of 1026 ± 68 HV, a deposition efficiency of 40% and a thickness of 265 ± 9.1 μm.

In comparison, the microstructures of coatings produced using different segmented configurations are displayed in Figure 4.

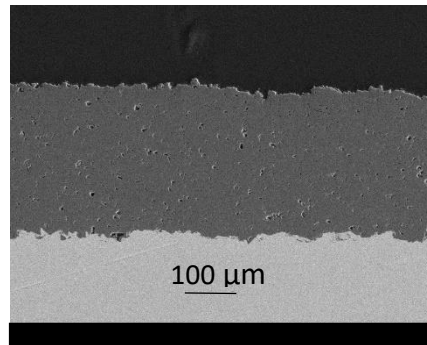


Figure 3: Microstructure of F4MB plasma-sprayed alumina coating

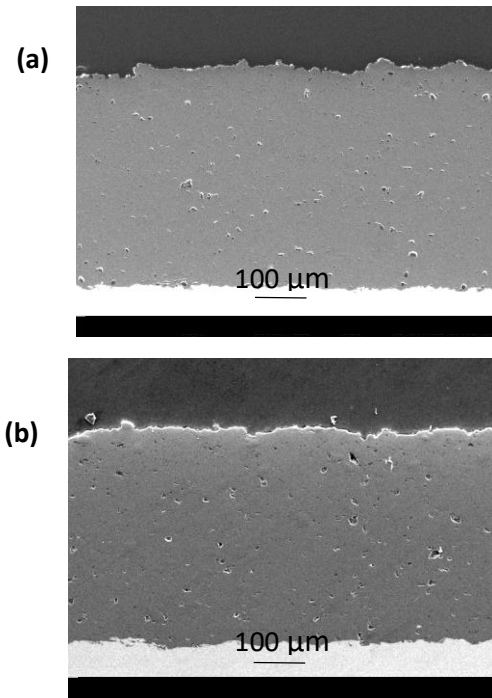


Figure 4: Microstructure of alumina coatings manufactured with (a) Larmor 9, (b) Larmor 15

Table 4 summarizes the microstructure characterization of the alumina coatings obtained by the Larmor segmented torches. Comparing these two to the reference coating show a reduction in porosity of less 1% vs 3% approximately, a higher hardness for the coating obtained with the segmented torches (> 1023 HV), a higher deposition yield (63 % vs 40 %) and a higher thickness (approximately 400 μm vs 260 μm).

Table 4: Properties of coatings

	F4MB	Larmor 9	Larmor 15
Porosity (%)	2.8	1	0.8
Hardness (HV)	1026 ± 68	1083 ± 120	1187 ± 66
Deposition efficiency (%)	40	63	53
Thickness (μm)	265 ± 9.1	420 ± 7.5	410 ± 9.4

3- Cost analysis

A comprehensive cost-benefit analysis is undertaken. This is because, even if a segmented torch uses more initial electrical power (71/82kW vs 51kW), it may offer advantages such as faster deposition times, increased layer thickness or improved spray efficiency, which can ultimately reduce overall processing costs. Additionally, as demonstrated in other studies, a reduction in the secondary hydrogen gas (H₂) flow rate minimizes electrode erosion [13]. Similarly, the presence of neutrodes, can also contribute to a reduced electrode wear. Therefore, based on these considerations, it can be concluded that these torches have the potential to decrease the overall process cost.

As seen before, with the Larmor torches, a higher thickness of the coating is obtained. So, to ensure a fair cost comparison, all deposits will be compared at the same thickness. The thickness considered is 350µm. The cost is calculated for an effective usage time (deposition time) for this thickness of coating (Table 5).

It should be noted, as mentioned previously, that the spraying is performed under the same net power.

Knowing the deposition time and electrical power, the energy calculation is based on the formula $E(\text{kWh}) = P(\text{kW}) \times t(\text{h})$, with P the initial electrical power and t the deposition time.

Table 5: Deposition time (min) and energy consumption for a thickness of 350 µm

Torches	Deposition time (s)	Initial electrical power (kW)	Energy (kWh)
Larmor 15	72	82	1.64
Larmor 9	70	71	1.38
F4MB	111	51	1.57

As seen in Table 5, the deposition time for a segmented torch is less compared to the F4MB one (111 s vs 70-72 s). The results in an energy used for deposition approximately similar for the three torches (1.4 - 1.6 kWh). In conclusion, the same amount of energy is used, independently of the torches used for coating manufacturing.

But as seen before the segmented torch uses lower amount of gas flow rate as presented in Table 6.

Table 6: Consumption of Ar and H₂ for the different respective deposition times

Torches	Deposition time (s)	Ar used (L)	H ₂ used (L)
Larmor 15	72	42	2.4
Larmor 9	70	41	2.3
F4MB	111	74	22.2

The calculation of the amount of used and wasted powder is presented in the following Table 7. Based on the presented results, the amount of powder wasted is less important for segmented torches than for the F4MB (12 vs. 31 g).

Table 7: Consumption and waste of the alumina powder for the considered deposition times

Torches	Deposition time (s)	Deposition efficiency (%)	Powder used (g)	Powder wasted (g)
Larmor 15	72	63	33.5	12.4
Larmor 9	70	63	32.7	12.1
F4MB	111	40	51.8	31.1

Although segmented torches employ a higher initial power setting, the reduced deposition time leads to equivalent energy consumption per deposition compared to the conventional torch. However, segmented torches offer a distinct advantage by utilizing less gas and powder during the deposition process.

To calculate the overall cost of the process, all the information in the previous tables must be taken into consideration: deposition time, energy consumed, quantity of powder used, and quantity of gas. The following costs, are taken from the laboratory's purchasing costs:

- 1 kWh = 0.2516 euro
- 1 L (Ar) = 0.00439 euro
- 1 L (H₂) = 0.00986 euro
- 1 g of Al₂O₃ powder = 0.02473 euro

Table 8 resumes the total cost for one spray. The cost process for only one-time deposition is smaller in the segmented torches (1.36-1.44 euro) than the conventional F4MB torch (2.22 euro).

So, for a longer time deposition, the segmented torches offer higher economic benefits with a cost reduction of about 62 %.

Table 8: total cost for one spray deposition

Torches	Electricity cost (euro)	Gas cost (euro)	Powder cost (euro)	Total cost (euro)
Larmor 15	1.63 x 0.25	42 x 0.00439 + 2.4 x 0.00986	33.5 x 0.02473	1.44
Larmor 9	1.38 x 0.25	41 x 0.00439 + 2.3 X 0.00986	32.7 x 0.02473	1.36
F4MB	1.57 x 0.25	74 x 0.00439 + 22.2 x 0.00986	51.8 x 0.02473	2.22

Conclusion

The results demonstrate that, for all three torches employed (F4MB: conventional torch, Larmor 9 and Larmor 15 segmented torches) with identical net powers, alumina coatings achieved with segmented torches exhibit equal or even superior characteristics. These advantages include increased hardness, reduced porosity, more efficient powder deposition and a greater layer thickness compared to the conventional torch.

Furthermore, segmented torches operate with a lower arc current and gas flow rates (Ar and H₂) compared to the F4MB one. So, this type of torches offers extended electrodes lifespan, resulting in reduced maintenance requirements.

Finally, the results also indicate that utilizing a segmented torch reduces deposition time, minimizes powder waste and generally decreases the overall cost of sample production.

Consequently, it can be concluded that segmented torches offer significant cost savings.

Perspectives

To achieve consistent net power output, parameters $I = 450\text{A}$, $\text{Ar} = 35\text{ L/min}$, and $\text{H}_2 = 2\text{ L/min}$ were established for the Larmor 9 tunnel 10 and Larmor 15 tunnel 10 torches. These parameters were determined through a series of experiments, as said before.

Complementary microstructural analyses of the deposits revealed consistent density (porosity < 1 %) and hardness ($\text{HV} > 1000$) across all torch types and parameters combinations. Building on this success, a follow-up study will investigate the possibility of further reducing deposition time while maintaining deposit quality using the same parameters but with an increased powder flow rate of 60 g/min.

Preliminary findings from this new study indicate slight variations in hardness (deposits at 60 g/min exhibit lower hardness) and thickness (deposits at 60 g/min are thicker). Porosity analysis is pending to determine its impact on deposit quality. If the results are positive, the powder flow rate will be further increased to 90 g/min, followed by a reevaluation of the deposits to establish the optimal process limit.

Acknowledgement

This work has been supported by the Bourgogne-Franche-Comté Region.

References

- [1] M. Kutz, Thermal spray coatings, in Handbook of Environmental Degradation of Materials (Third Edition). 2018, Elsevier, p. 469-488.
- [2] P. L. Fauchais, J. V. R. Heberlein, and M. I. Boulos, Thermal Spray Fundamentals: From Powder to Part. Boston, MA: Springer US, 2014. doi: 10.1007/978-0-387-68991-3.
- [3] Z. Duan and J. Heberlein, "Arc Instabilities in a Plasma Spray Torch," J. Therm. Spray Technol., vol. 11, no. 1, pp. 44–51, Mar. 2002, doi: 10.1361/105996302770348961.
- [4] V. Rat, F. Mavier, and J. F. Coudert, "Electric Arc Fluctuations in DC Plasma Spray Torch," Plasma Chem. Plasma Process., vol. 37, no. 3, pp. 549–580, May 2017, doi: 10.1007/s11090-017-9797-7.
- [5] J. F. Coudert, M. P. Planche, and P. Fauchais, "Characterization of d.c. plasma torch voltage fluctuations," Plasma Chem. Plasma Process., vol. 16, no. S1, pp. S211–S227, Mar. 1995, doi: 10.1007/BF01512636.
- [6] L. An, Y. Gao, and C. Sun, "Effects of Anode Arc Root Fluctuation on Coating Quality During Plasma Spraying," J. Therm. Spray Technol., vol. 20, no. 4, pp. 775–781, Jun. 2011, doi: 10.1007/s11666-011-9644-y.
- [7] B. Bora, N. Aomoa, and M. Kakati, "Characteristics and Temperature Measurement of a Non-Transferred Cascaded DC Plasma Torch," Plasma Sci. Technol., vol. 12, no. 2, pp. 181–187, Apr. 2010, doi: 10.1088/1009-0630/12/2/11.
- [8] J. Schein, M. Richter, K. D. Landes, G. Forster, J. Zierhut, and M. Dzulko, "Tomographic Investigation of Plasma Jets Produced by Multielectrode Plasma Torches," J. Therm. Spray Technol., vol. 17, no. 3, pp. 338–343, Sep. 2008, doi: 10.1007/s11666-008-9186-0.
- [9] D. Chen, R. Rocchio-Heller, and C. Dambra, "Segmented Thermal Barrier Coatings for ID and OD Components Using the SinplexPro Plasma Torch," J. Therm. Spray Technol., vol. 28, no. 7, pp. 1664–1673, Oct. 2019, doi: 10.1007/s11666-019-00920-x.
- [10] A. Dolmaire et al., "Benefits of Hydrogen in a Segmented-Anode Plasma Torch in Suspension Plasma Spraying," J. Therm. Spray Technol., vol. 30, no. 1–2, pp. 236–250, Jan. 2021, doi: 10.1007/s11666-020-01134-2.
- [11] G. Darut, M. P. Planche, H. Liao, C. Adam, A. Salito, and M. Rösli, "Study of the In-Flight Characteristics of Particles for Different Configurations of Cascade Plasma Torches," presented at the ITSC2021, F. Azarmi, X. Chen, J. Cizek, C. Cojocar, B. Jodoin, H. Koivuluoto, Y. C. Lau, R. Fernandez, O. Ozdemir, H. Salimi Jazi, and F. Toma, Eds., Virtual, Jun. 2021, pp. 499–507. doi: 10.31399/asm.cp.itsc2021p0499.
- [12] "ImageJ. Available online: <http://imagej.nih.gov/ij/> (accessed on 3 May 2024)."

[13] P. Fauchais, "Understanding plasma spraying," *J. Phys. Appl. Phys.*, vol. 37, no. 9, pp. R413–R414, May 2004, doi: 10.1088/0022-3727/37/9/R02.